

# Low-Density Lipoprotein Uptake Inhibits the Activation and Antitumor Functions of Human V $\gamma$ 9V $\delta$ 2 T Cells

Neidy V. Rodrigues<sup>1,2,3,4</sup>, Daniel V. Correia<sup>1</sup>, Sofia Mensurado<sup>1</sup>, Sandrina Nóbrega-Pereira<sup>1</sup>, Ana deBarros<sup>1</sup>, Fernanda Kyle-Cezar<sup>5</sup>, Andrew Tutt<sup>5,6</sup>, Adrian C. Hayday<sup>5,7</sup>, Haakan Norell<sup>1</sup>, Bruno Silva-Santos<sup>1</sup>, and Sérgio Dias<sup>1</sup>



## Abstract

V $\gamma$ 9V $\delta$ 2 T cells, the main subset of  $\gamma\delta$  T lymphocytes in human peripheral blood, are endowed with antitumor functions such as cytotoxicity and IFN $\gamma$  production. These functions are triggered upon T-cell receptor–dependent activation by non-peptidic prenyl pyrophosphates ("phosphoantigens") that are selective agonists of V $\gamma$ 9V $\delta$ 2 T cells, and which have been evaluated in clinical studies. Because phosphoantigens have shown interindividual variation in V $\gamma$ 9V $\delta$ 2 T-cell activities, we asked whether metabolic resources, namely lipids such as cholesterol, could affect phosphoantigen-mediated V $\gamma$ 9V $\delta$ 2 T-cell activation and function. We show here that V $\gamma$ 9V $\delta$ 2 T cells express the LDL receptor upon activation and take up LDL cholesterol. Resulting

changes, such as decreased mitochondrial mass and reduced ATP production, correlate with downregulation of V $\gamma$ 9V $\delta$ 2 T-cell activation and functionality. In particular, the expression of IFN $\gamma$ , NKG2D, and DNAM-1 were reduced upon LDL cholesterol treatment of phosphoantigen-expanded V $\gamma$ 9V $\delta$ 2 T cells. As a result, their capacity to target breast cancer cells was compromised both *in vitro* and in an *in vivo* xenograft mouse model. Thus, this study describes the role of LDL cholesterol as an inhibitor of the antitumor functions of phosphoantigen-activated V $\gamma$ 9V $\delta$ 2 T cells. Our observations have implications for therapeutic applications dependent on V $\gamma$ 9V $\delta$ 2 T cells. *Cancer Immunol Res*; 6(4); 448–57. ©2018 AACR.

## Introduction

Among the lymphocyte populations being considered for cancer immunotherapy are  $\gamma\delta$  T cells, which display antitumor functions such as cytotoxicity and IFN $\gamma$  production upon activation (1, 2). In humans and other primates, most (70%–95%)  $\gamma\delta$  peripheral blood lymphocytes (PBLs) express heterodimers of V $\gamma$ 9 and V $\delta$ 2 chains. These V $\gamma$ 9V $\delta$ 2 T cells recognize and kill cells from a variety of tumor types, such as melanoma, leukemia, lymphoma, lung, ovary, and breast cancers. This cytotoxicity does not require antigen processing or MHC-mediated antigen presentation (3, 4). Instead, V $\gamma$ 9V $\delta$ 2 T cells are activated by small non-peptidic prenyl-pyrophos-

phate metabolites of isoprenoid biosynthesis, termed phosphoantigens (PAGs), in a T-cell receptor (TCR)–dependent but MHC-independent manner (5, 6). Phosphoantigens interact with an intracellular domain of butyrophilin-3A1 (BTN3A1; CD277), a B7 superfamily member that provides the extracellular motifs recognized by V $\gamma$ 9V $\delta$ 2 TCRs (7–9). V $\gamma$ 9V $\delta$ 2 TCRs are enriched for public V $\gamma$ 9JP<sup>+</sup> sequences (10) that may account for their "innate-like" (i.e., fast) kinetics of response to PAGs. Although the most potent PAGs derive from the non-mevalonate pathway of bacteria and parasites, tumor cells accumulate metabolite intermediates of the mevalonate pathway [e.g., isopentenyl pyrophosphate (IPP)] that also activate primate V $\gamma$ 9V $\delta$ 2 T cells (5, 11, 12).

Like TCRs, NK cell receptors, particularly NKG2D and DNAM-1, contribute to tumor cell recognition and targeting by V $\gamma$ 9V $\delta$ 2 T cells. The receptor NKG2D is required for recognition of leukemia and lymphoma cells by phosphoantigen-activated V $\gamma$ 9V $\delta$ 2 T cells where ULBP1 is the dominant NKG2D ligand expressed on the target cells (13). Other NKG2D ligands, namely MICA (14) and ULBP4 (15), are implicated in NKG2D-mediated recognition of multiple myeloma, ovarian, and colon carcinoma (16). The DNAM-1 ligands, including Nectin-like-5 and Nectin-2, underlie hepatocellular carcinoma (HCC) cell targeting by V $\gamma$ 9V $\delta$ 2 T cells (17). We have therefore proposed that NK receptors determine antitumor cytotoxicity of phosphoantigen-activated V $\gamma$ 9V $\delta$ 2 T cells (18).

Several attributes of V $\gamma$ 9V $\delta$ 2 T cells have prompted their use in the clinic (19): (i) their antitumor properties, (ii) their lack of reliance on MHC class I presentation, a common immune evasion mechanism, and (iii) their independence of mutated epitopes,

<sup>1</sup>Instituto de Medicina Molecular, Faculdade de Medicina, Universidade de Lisboa, Portugal. <sup>2</sup>Instituto Gulbenkian de Ciência, Oeiras, Portugal. <sup>3</sup>Programa de Pós-Graduação Ciência para o Desenvolvimento, Oeiras, Portugal. <sup>4</sup>Faculdade de Ciência e Tecnologia, Uni-CV, Campus do Palmarejo, Praia, Cabo Verde. <sup>5</sup>King's College London, London, United Kingdom. <sup>6</sup>Institute of Cancer Research, London, United Kingdom. <sup>7</sup>Francis Crick Institute, London, United Kingdom.

**Note:** Supplementary data for this article are available at Cancer Immunology Research Online (<http://cancerimmunolres.aacrjournals.org/>).

B. Silva-Santos and S. Dias contributed equally to this article.

**Corresponding Authors:** Sérgio Dias, Edifício Egas Moniz, Faculdade de Medicina da Univ. Lisboa, 1649-028 Lisboa, Portugal. Phone: 351-217-999-411; Fax: 351-217-999 411; E-mail: sergiodias@fm.ul.pt; and Bruno Silva-Santos, E-mail: bssantos@medicina.ulisboa.pt

**doi:** 10.1158/2326-6066.CIR-17-0327

©2018 American Association for Cancer Research.

which makes V $\gamma$ 9V $\delta$ 2 T cells effective against tumors with low mutation loads. Most clinical trials have selectively activated and expanded V $\gamma$ 9V $\delta$ 2 T cells with use of the chemical aminobisphosphonates, including pamidronate and zoledronate, which are approved by the FDA for treatment of osteoporosis and bone metastases. These drugs interfere with PAg-processing enzymes and increase the intracellular levels of IPP in tumor cells (20). The synthetic PAg, bromohydrin pyrophosphate (BrHPP), has been used *in vivo* and *ex vivo* to activate and expand autologous V $\gamma$ 9V $\delta$ 2 T cells for reinfusion. However, the clinical performance of V $\gamma$ 9V $\delta$ 2 T cells has been disappointing thus far. Moreover, the prognostic value of V $\gamma$ 9V $\delta$ 2 (or total  $\gamma\delta$ ) T-cell infiltration in tumors has been found variable, such that correlations with patient outcome range from positive (melanoma) to neutral (renal cancer) to negative (breast cancer and colorectal cancer; ref. 21). A bioinformatics study surveying ~10,000 cancer biopsies from 50 types of hematologic and solid malignancies described considerable interindividual variation of V $\gamma$ 9V $\delta$ 2 tumor-infiltrating lymphocyte (TIL) abundance that reflected in variable associations with outcome (22).

Although many factors could underlie the interindividual variation of V $\gamma$ 9V $\delta$ 2 T-cell activities, studies indicate that metabolic resources, namely lipids such as cholesterol, could affect V $\gamma$ 9V $\delta$ 2 T-cell activation and functions (23–27). Cholesterol, an essential component of membranes, regulates membrane fluidity and thus affects various receptor-mediated signal transduction pathways. Inhibition of cholesterol esterification or deletion of the responsible genes in CD8<sup>+</sup> T cells increases the amount of cholesterol in the plasma membrane and enhances TCR signaling, promoting cytotoxic functions and proliferation (28). Genetic interference with cholesterol efflux via the ABCG1 transporter converted "pro-tumor" M2 macrophages into antitumor M1 macrophages and suppressed tumor growth (29). Immune cell functions can thus be affected by alterations in cholesterol homeostasis (25). On the other hand, systemic cholesterol favors breast cancer progression by promoting breast cancer cell proliferation, migration and survival (30). LDL cholesterol level in breast cancer patients has predictive value at the time of diagnosis: women with elevated LDL cholesterol levels at diagnosis have a higher risk of developing local recurrence or metastasis.

In this study, we asked whether LDL affects V $\gamma$ 9V $\delta$ 2 T-cell activation and targeting toward breast cancer cells. We found that activated V $\gamma$ 9V $\delta$ 2 T cells express LDL-R through which they take up LDL cholesterol. The LDL cholesterol uptake drives metabolic changes associated with reduced functionality, namely impaired IFN $\gamma$  production and reduced killing of breast cancer cells both *in vitro* and *in vivo*. This work thus demonstrates that LDL cholesterol levels modulate V $\gamma$ 9V $\delta$ 2 T-cell activation and antitumor functions.

## Materials and Methods

### Cell culture and *in vitro* killing assays

For V $\gamma$ 9V $\delta$ 2 T-cell culture and expansion, peripheral blood mononuclear cells were isolated by density gradient centrifugation (Ficoll-Hystopaque-1077; Sigma-Aldrich) for 30 minutes at 1,500 rpm and 25°C. V $\gamma$ 9V $\delta$ 2 T cells were cultured in RPMI 1640 medium supplemented with 10% FBS and 50  $\mu$ g/mL of penicillin/streptomycin (Invitrogen, Gibco), in the presence of interleukin-2 (IL2; Peprotech) and (E)-4-hydroxy-3-methyl-but-2-enyl pyrophosphate (HMB-PP; Echelon Biosciences). Fresh medium was added every 5 days, until day 14 of culture. Expanded V $\gamma$ 9V $\delta$ 2

T-cell populations were cultured for 36 to 72 hours at 37°C and 5% CO<sub>2</sub> in the presence or in the absence of low density human lipoproteins (LDL; 100  $\mu$ g/mL, Millipore), and tested for their antitumor activity. Cells were counted in Neubauer chamber using 0.4% Trypan Blue solution (Sigma-Aldrich) for viability control.

For tumor cell cultures and *in vitro* killing assays, the human breast cancer cell line MDA-MB-231 (ATCC) was cultured in DMEM medium (Gibco Invitrogen) supplemented with 10% heat-inactivated fetal bovine serum (FBS, Gibco Invitrogen) and 1% penicillin–streptomycin (Life Technologies). Cell lines were not reauthenticated in the past year. *In vitro*-expanded V $\gamma$ 9V $\delta$ 2 T cells were seeded in 96-well round-bottom plates. Tumor cells were stained with CellTrace Far Red DDAO-SE (1  $\mu$ mol/L; Molecular Probes; Invitrogen) and incubated at the indicated target: effector ratio with V $\gamma$ 9V $\delta$ 2 T cells for 3 hours at 37°C and 5% CO<sub>2</sub>. Cells were then stained with Annexin V-FITC (BD Pharmingen) and analyzed by flow cytometry.

For receptor blocking, cultured V $\gamma$ 9V $\delta$ 2 T cells were preincubated for 1 hour with saturating amounts of blocking antibodies; human anti-TCR- $\gamma\delta$  (clone B1), human anti-NKG2D (clone 1D11), human anti DNAM-1 (11A8), human anti-FasL (clone NOK-1), human anti-CD2 (clone RPA-2.10), human-anti 2B4 (C1.7), mouse IG3k (clone MG3-35), all from Biolegend. Blocking antibodies were maintained in the culture medium during the killing assays.

### Flow-cytometry analysis

For cell surface protein staining, cells were labeled with fluorescent monoclonal antibodies: anti-CD3 (clone UCHT1, Biolegend), anti-CD45 (HI30, Biolegend), anti-CD69 (FN50, Biolegend), anti-TcRV $\gamma$ 9 (clone B3, Biolegend), anti-TcRV $\delta$ 2 (clone B6, Biolegend), anti-LDL-R (FAB2148A, R&D Systems), anti-NKG2D (clone 1D11, Biolegend), anti-DNAM-1 (clone 11A8, Biolegend), anti-CD56 (clone HCD56, Biolegend), anti-CD279 (PD-1) NAT105, Biolegend). In all cultures, the percentage of V $\gamma$ 9<sup>+</sup> T cells was evaluated by flow cytometry in a LSR Fortessa (BD Biosciences) flow cytometer.

For lipid droplet determination, expanded V $\gamma$ 9V $\delta$ 2 T cells were stained with 0.5 to 1.5  $\mu$ g/mL Nile Red (Sigma-Aldrich), followed by 10 minutes of incubation in the dark at room temperature (RT) and analysis in a LSR Fortessa flow cytometer. Alternatively, lipid droplet quantification was done using V $\gamma$ 9V $\delta$ 2 T cells preincubated for 10 minutes with 3.8 mmol/L Bodipy (Invitrogen) at RT, washed twice with PBS, and then analyzes in a LSR Fortessa flow cytometer. For ROS quantification, cultured V $\gamma$ 9V $\delta$ 2 T cells were stained with 1 to 10  $\mu$ mol/L ROS-CH-H2DFDA (ThermoFisher Scientific) fluorescent dyes for 30 minutes at 37°C, washed twice and analyzed by flow cytometry (BD LSR Fortessa flow cytometer). For determination of mitochondrial mass, cultured V $\gamma$ 9V $\delta$ 2 T cells were washed with PBS and preincubated for 15 minutes with 2 nmol/L MitoTracker Deep Red (Molecular Probes) at RT, washed again with PBS, then analyzed in LSR Fortessa flow cytometer. For cell proliferation, cultured V $\gamma$ 9V $\delta$ 2 T cells were stained with CFSE (CellTrace CFSE Cell Proliferation Kit, Invitrogen) at 0.5  $\mu$ mol/L. Cell death *in vitro* was assessed by Annexin V-FITC (BD Pharmingen) staining, where cultured V $\gamma$ 9V $\delta$ 2 T cells were washed in PBS and resuspended in 300  $\mu$ L Annexin V binding buffer (BD Biosciences) containing Annexin V-FITC (BD Pharmingen), and incubated for 15 minutes at RT before analysis in an LSR Fortessa flow cytometer. For cytokine detection, cultured V $\gamma$ 9V $\delta$ 2 T cells were fixed in 25 ng/mL PMA (Sigma Aldrich,

P-8138), 2 µg/mL Ionomycin (Sigma, I-0634) and 2 µg/mL Brefeldin-A (Sigma, B-7651) in RPMI medium for 4 hours at 37°C. For cell surface staining, Vγ9Vδ2 T cells were washed and stained with fluorescent antibodies for 10 minutes at 4°C. For intracellular staining, cells were then resuspended in fix/permeabilization buffer (BD Biosciences) and incubated for 30 minutes at 4°C, followed by incubation in permeabilization buffer with Fc-block (1:100) for 15 minutes. Antibodies for intracellular staining were added (1:100) for 30 minutes at 37°C and 5% CO<sub>2</sub>. Concentrations of IFNγ (B27), TNFα (Mab-11), and IL17A (BL-168) were assayed in an LSR Fortessa cytometer by flow (BD Biosciences).

#### Quantitative real-time PCR

RNA was extracted from cultured Vγ9Vδ2 T cells using TRIzol reagent (Invitrogen) according to the manufacturer's protocol. Concentration was determined by spectrophotometry (Nanodrop 1000) and total RNA was reverse-transcribed into cDNA using random hexamers and Superscript II enzyme (Invitrogen). Quantitative real-time PCR (qPCR) was performed using Sybr-Green reagent (Bio-Rad) in a ViiA 7 System sequence detection system (Applied Biosystems). Quantifications were done by applying the ΔCt method [(Ct of gene of interest) – (Ct of housekeeping gene)] followed by 2<sup>(-ΔΔCt)</sup>. The housekeeping gene used for input normalization was β-2 microglobulin. Primers used in the quantitative PCR assays were: LDL-R, Fwd: 5'-GCTTGCTGTACCTGCAAA-3'; LDL-R, Rev: 5'-AACTGCCGAGAGATGCACTT-3'; CD69, Fwd: 5'-CAAGTTCCTGTCTGTG-TGC-3'; CD69, Rev: 5'-GAGAATGTGTATTGGCCTGGA-3'; IFNγ, Fwd: 5'GGCATTGAAGAATTGGAAG-3'; IFNγ, Rev: 5'-TTTGATGCTCTGGTCATCTT-3'; FASL, Fwd: 5'-GTTCTGGTTGCC-TTGGTAGG-3'; FASL, Rev: 5'-TGTGCATCTGGCTGCTAGAC-3'; STAT1, FW: 5'-AGTTCGGCAGCAGCTTAAA-3'; STAT1, Rev: 5'-TGCTTTCCACCACAAACGA-3'; IL10, Fwd: CCAGTCTGAGAA-CAGCTGCAC-3'; IL10, Rev: 5'-GCTGAAGGCATCTCGGA-GAT-3'.

For mtDNA determination, expanded Vγ9Vδ2 T cells (1 × 10<sup>6</sup> cells/mL) were resuspended with protein K and incubated at 65°C for 3 hours with vertical rotation. Total DNA was isolated from cells using phenol:chloroform:isoamyl alcohol (Sigma) and measured by assessing the levels of the human mitochondrial ND1 (human mtND1: 5'-CCCTAAAACCCGCCACATCT-3' and 5'-GAGCGATGGTGAAGCTAAGGT-3') relative to nuclear β2-microglobulin gene (5'-TCGCTCCGTGGCCTTAGCTGT-3' and 5'-CTTTGGAGTACGCTGGATAGCCTCC-3') using SybrGreen reagent (Bio-Rad) and ViiA 7 System sequence detection system (Applied Biosystems). Quantifications were made applying the ΔCt method [(Ct of nuclear DNA gene) – (Ct of mitochondrial DNA gene)] followed by 2 × 2<sup>(ΔCt)</sup> according to others (31).

#### Histologic analysis

For detection of lipid droplets, poly-lysine was used to coat slides and promote attachment of Vγ9Vδ2 T cells. Then, Vγ9Vδ2 T cells were fixed with 4% paraformaldehyde in PBS for 15 minutes and stained with 0.1 µg/mL Bodipy (Invitrogen) in PBS, at RT for 15 minutes. Cells were washed three times with PBS and mounted with Vectashield mounting medium containing DAPI (Vector Laboratories). Images were captured using a Zeiss LSM710 confocal microscope.

The immunohistologic staining for Ki67 (MIB-1) and human CD3 in subcutaneous tumors were performed in 4-µm sections

following conventional protocols. Briefly, for antigen retrieval, the slides were treated in a PT Link module (DAKO) at low-pH, followed by incubation with the primary antibodies. EnVision Link horseradish peroxidase/DAB visualization system (DAKO) was used and counterstained with Harris hematoxylin. Slides were scanned in the Hamamatsu NanoZoomerSQ.

#### In vivo tumor experiments

All animal experiments were performed in accordance with national guidelines from the "Direção Geral de Veterinária" and approved by the National Ethics Committee. NSG mice were obtained from The Jackson Laboratories. Female mice (ages 5–7 weeks) were injected with MDA-MB-231 Luciferase-GFP (pre-transduced with a lentiviral vector encoding luciferase and GFP and enriched for GFP<sup>+</sup> cells) breast cancer cells in the right axillary mammary fat pad and, after the tumor was established (day 17), Vγ9Vδ2 T cells or PBS (control) were injected twice. After 19 days of treatment, animals were sacrificed and organ, tumor, and blood were collected for further analysis.

#### Statistical analysis

*In vitro* and *in vivo* data are presented as the mean ± SD. Statistical analyses were performed using Student *t* test or ANOVA. Unpaired Student *t* test and one-way analysis of variance were used for comparison of experimental groups. Statistical analysis was performed using GraphPad Prism software version 6.

## Results

### Activated Vγ9Vδ2 T cells take up LDL via LDL receptor

We started this study by investigating the capacity of Vγ9Vδ2 T cells to sense and take up native LDL cholesterol. For this purpose, we activated and expanded γδ T cells *in vitro* for up to 14 days with IL2 plus the most potent phosphoantigen, hydroxyl-methyl-butynyl pyrophosphate (HMB-PP), which resulted in a cell population of which ~80% were Vδ2<sup>+</sup> T cells (Supplementary Fig. S1A). This type of cellular product has therapeutic relevance and is being used in adoptive cell transfer (19). In our flow cytometry analyses, we set our gates on Vδ2<sup>+</sup> T cells to avoid contamination by other cell types. We will thus refer herein to this phosphoantigen-activated and Vγ9Vδ2 T cell-enriched cellular product simply as "activated Vγ9Vδ2 T cells." We exposed these cells for 36 to 72 hours to LDL cholesterol (in the same culture medium used for the expansion) and used Bodipy 493/503 and Nile Red to document internalization and intracellular accumulation of cholesterol (Fig. 1A–C). Cholesterol accumulated at 100 µg/mL but not at 50 µg/mL LDL cholesterol concentration, and thus we used 100 µg/mL LDL cholesterol for all subsequent experiments. Although Vδ2<sup>+</sup> (or Vδ1<sup>+</sup>) T cells rarely expressed the LDL cholesterol receptor (LDL-R; Supplementary Fig. S1B) *ex vivo* or in the tumor environment (Supplementary Fig. S1C), Vγ9Vδ2 T cells expressed (~30%) LDL-R upon activation (Fig. 1D; Supplementary Fig. S1D). The association of LDL-R expression with Vγ9Vδ2 T-cell activation was further documented by the cosegregation of expression with the activation marker CD69 (Fig. 1D). Non-Vδ2<sup>+</sup> cells within the cultures, including Vδ1<sup>+</sup> T cells, failed to increase their lipid content (Supplementary Fig. S1E). We conclude that only activated Vγ9Vδ2 T cells take up LDL cholesterol in these cultures.

Exposure of activated Vγ9Vδ2 T cells to LDL led to a down-regulation of LDL-R expression (Fig. 1E), suggestive of receptor internalization. LDL-R blockade with monoclonal antibodies

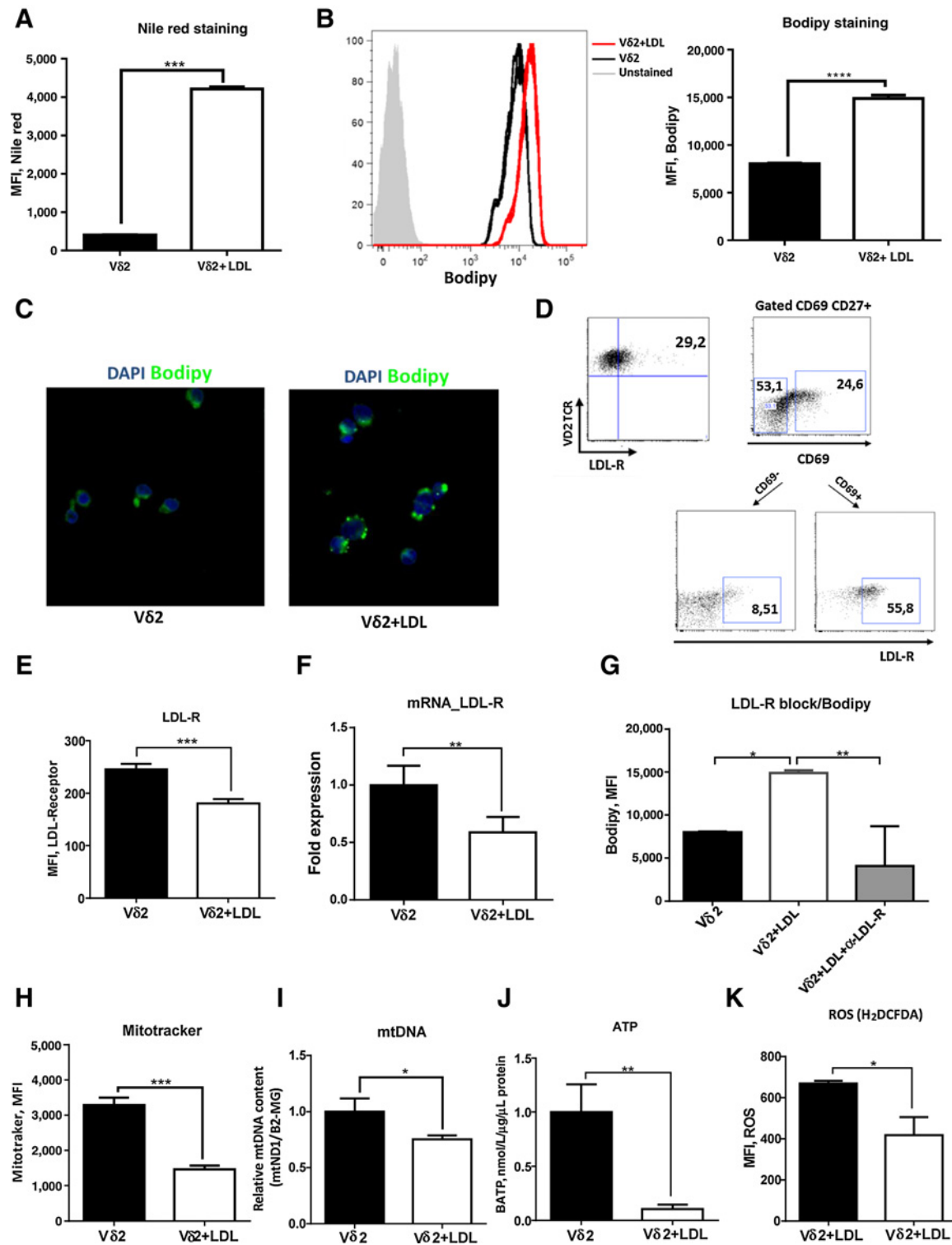


**Figure 1.**

Activated  $\gamma\delta$  T cells take up LDL cholesterol via LDL-R. Activated and expanded  $\gamma\delta$  (~80% V $\delta$ 2<sup>+</sup>) T cells were cultured in RPMI 1640 medium with IL2 and HMB-PP [(E)-4-hydroxy-3-methyl-but-2-enyl pyrophosphate] in the absence (V $\delta$ 2) or presence of LDL cholesterol (V $\delta$ 2+LDL) for 72 hours. LDL cholesterol uptake was assessed by Nile red (A) and Bodipy (B and C) lipid droplet staining by flow cytometry. D, Flow cytometry plots for control (in the absence of LDL treatment) LDL-R expression in gated V $\delta$ 2<sup>+</sup> T cells (left) or segregated on the basis of CD69 expression (right). E, Mean fluorescence intensity (MFI) for LDL-R expression on V $\delta$ 2<sup>+</sup> T cells after 72 hours of incubation in the absence (V $\delta$ 2) or presence of LDL cholesterol (V $\delta$ 2 + LDL). F, RT-qPCR analysis of the mRNA expression of *LDL-R*, normalized to the housekeeping gene  $\beta$ 2-microglobulin. G, MFI for Bodipy lipid droplet staining in expanded V $\delta$ 2<sup>+</sup> T cells, cultured in the presence of LDL only or in the presence of an anti-LDL-R. H-J, Mitochondrial mass was measured by MitoTracker Deep Red staining (H), relative mitochondrial DNA (mtDNA) content determined by qPCR quantification in DNA samples (I), ATP production (J), and reactive oxygen species (ROS) content by H<sub>2</sub>DCFDA staining (K) in cell extracts obtained as in E. Data are from three independent experiments and are presented as mean  $\pm$  SD. \*,  $P < 0.05$ ; \*\*,  $P < 0.01$ ; \*\*\*,  $P < 0.001$ .

inhibited accumulation of cholesterol in V $\gamma$ 9V $\delta$ 2 T cells (Fig. 1F). These data demonstrate that LDL-R expression endows activated V $\gamma$ 9V $\delta$ 2 T cells with the capacity to take up LDL cholesterol.

We next characterized the effects of LDL exposure and uptake on metabolism of V $\gamma$ 9V $\delta$ 2 T cells. We observed reduced mitochondrial mass (Fig. 1H), mitochondrial DNA content (Fig. 1I), decreased cellular ATP levels (Fig. 1J), and production of reactive oxygen species (Fig. 1K), in V $\gamma$ 9V $\delta$ 2 T cells exposed to LDL cholesterol. The effects of LDL cholesterol were not accompanied by a decrease in cell viability, as demonstrated by quantification of apoptosis of V $\gamma$ 9V $\delta$ 2 T cells exposed (or not) to LDL (Supplementary Fig. S1F). Thus, LDL cholesterol uptake affected the metabolic output of V $\gamma$ 9V $\delta$ 2 T cells.

#### LDL uptake inhibits V $\gamma$ 9V $\delta$ 2 T-cell activation and cytokine production

Activated V $\gamma$ 9V $\delta$ 2 T cells express the surface marker CD69 and produce cytotoxic and proinflammatory cytokines (5–7). Here, we tested whether these functional properties were affected by LDL cholesterol uptake over a 72-hour period in which preexpanded/activated V $\gamma$ 9V $\delta$ 2 T cells were incubated with medium alone, IL2 or IL2 + HMB-PP. We observed a decrease in the proportion of CD69<sup>+</sup> cells (Fig. 2A; Supplementary Fig. S2), as well as CD69 protein (Fig. 2B) and mRNA (Fig. 2C) expression levels in V $\gamma$ 9V $\delta$ 2 T cells upon exposure to LDL cholesterol. The impairment in CD69 expression was partially reverted by LDL-R blockade or treatment with nystatin (Fig. 2B), which sequesters cellular cholesterol when used in *in vitro* assays. CD3 expression was also downregulated (Fig. 2D). LDL cholesterol uptake affected expression of both IFN $\gamma$  protein and mRNA (Fig. 2E and F), the latter associating with a downregulation of the transcriptional regulator of IFN $\gamma$  expression, Stat-1 (Fig. 2G). Other functional properties, such as TNF $\alpha$ , IL17 or IL10 production, were not affected by LDL exposure (Supplementary Fig. S3). These data demonstrate that LDL cholesterol uptake limits activation of V $\gamma$ 9V $\delta$ 2 T cells as well as their capacity to produce their antitumor cytokine, IFN $\gamma$ .

#### LDL downregulates NKG2D and DNAM-1 and reduces $\gamma\delta$ T-cell cytotoxicity *in vitro*

Activated V $\gamma$ 9V $\delta$ 2 T cells killed the breast cancer cell line MDA-MB-231 in a dose-dependent manner. Exposure to LDL cholesterol inhibited this cytotoxic function (Fig. 3A). V $\gamma$ 9V $\delta$ 2 T cells exposed to LDL cholesterol also showed reduced expression of the cytotoxicity-associated marker, CD56, in preexpanded/activated V $\gamma$ 9V $\delta$ 2 T cells kept on IL2 alone or HMB-PP plus IL2 (Fig. 3B). To study the mechanism, we assessed two determinants of antitumor V $\gamma$ 9V $\delta$ 2 T-cell cytotoxicity, NKG2D (16) and DNAM-1 (17). Exposure to LDL cholesterol compromised expression of both receptors in the presence of serum (Fig. 3C; Supplementary Fig. S2) or human plasma (Supplementary Fig. S4). Serum or plasma was required for MDA-MB-231 cell targeting by preactivated V $\gamma$ 9V $\delta$ 2 T cells, as demonstrated by antibody blockade during the *in vitro* killing assay (Fig. 3D). NKG2D and DNAM-1 synergized in tumor cell recognition, because the blockade of each individual receptor had no effect on the killing assay (Supplementary Fig. S5). In addition, LDL cholesterol exposure prevented effects from NKG2D/ DNAM-1 blockade, further supporting the role of these receptors in the cytotoxic mechanisms impaired in

V $\gamma$ 9V $\delta$ 2 T cells (Fig. 3E). We concluded that LDL cholesterol uptake contributes to antitumor cytotoxicity, which prompted us to test the functionality of LDL cholesterol-exposed V $\gamma$ 9V $\delta$ 2 T cells in an *in vivo* breast cancer model.

#### LDL limits the antitumor therapeutic effect of human $\gamma\delta$ T cells *in vivo*

We used immunodeficient mice (NSG) injected with the human breast cancer cell line MDA-MB-231luc<sup>+</sup> (expressing luciferase) to test the therapeutic potential of adoptive transfer of V $\gamma$ 9V $\delta$ 2 T cells with or without previous exposure to LDL cholesterol. First, we used flow cytometry and immunohistochemistry to confirm that human (CD3<sup>+</sup>) T cells could be detected in blood of inoculated mice (Fig. 4A) and could infiltrate tumors (Fig. 4A and B). LDL cholesterol treatment did not affect human T-cell abundance either in the blood or within the tumor, showing that LDL exposure does not impact implantation, expansion or migration capacities of human T cells (Fig. 4A and B). However, LDL cholesterol -exposed T cells were less effective at controlling tumor growth than were V $\gamma$ 9V $\delta$ 2 T cells that had not been exposed to LDL cholesterol (Fig. 4C and D). In fact, LDL exposed V $\gamma$ 9V $\delta$ 2 T cells had no therapeutic impact (as compared with the PBS-injected control group; Fig. 4C and D). These data demonstrate that LDL cholesterol uptake has a negative impact on V $\gamma$ 9V $\delta$ 2 T-cell activation, which results in impaired antitumor functions *in vivo*.

## Discussion

Altered lipid metabolism is a hallmark of cancer (32). This metabolic change is modulated by oncogenic signaling pathways and promotes tumor initiation and progression, because cellular growth is dependent on the sustained availability of lipids (33). Moreover, metabolic shifts in lipid metabolism drive tumor recurrence after therapeutic intervention (34). Alterations in *de novo* lipid biosynthesis are associated with cancer pathogenesis (35). Uptake of exogenous lipids by tumor cells and by nonmalignant cells in the tumor microenvironment may also contribute to malignancy (36–38). This particular metabolic feature may explain the association of some cancers, including breast cancer, with diets high in fat or cholesterol (39).

Cholesterol is an essential component of cell membrane microdomains, including lipid rafts (40). As such, cholesterol is essential for the activation of signal transduction pathways, intracellular trafficking, polarity and cell migration. We and others have shown that LDL cholesterol favors breast cancer growth by directly modulating cancer cell properties (23, 30). On the other hand, genetic interference with cholesterol efflux (via the ABCG1 transporter) converts "pro-tumor" M2 macrophages into antitumor M1 macrophages and suppress tumor growth (41). However, it remained to be addressed whether LDL cholesterol had additional roles on TILs or on cellular products to be used for adoptive cell therapy (ACT) of cancer. In the present study, we investigated whether LDL cholesterol affected the activation and antitumor activity of human V $\gamma$ 9V $\delta$ 2 T cells, which hold promise for ACT. We found that LDL is internalized and accumulates in V $\gamma$ 9V $\delta$ 2 T cells, leading to reduce V $\gamma$ 9V $\delta$ 2 T-cell activation, mitochondrial mass and ATP production. LDL-exposed V $\gamma$ 9V $\delta$ 2 T cells show reduced antitumor function *in vitro* and *in vivo* (in a xenograft model of human breast cancer).

Cholesterol metabolism seems to mediate T-cell function. LDL-R is pivotal to cellular regulation. LDL-R downregulation

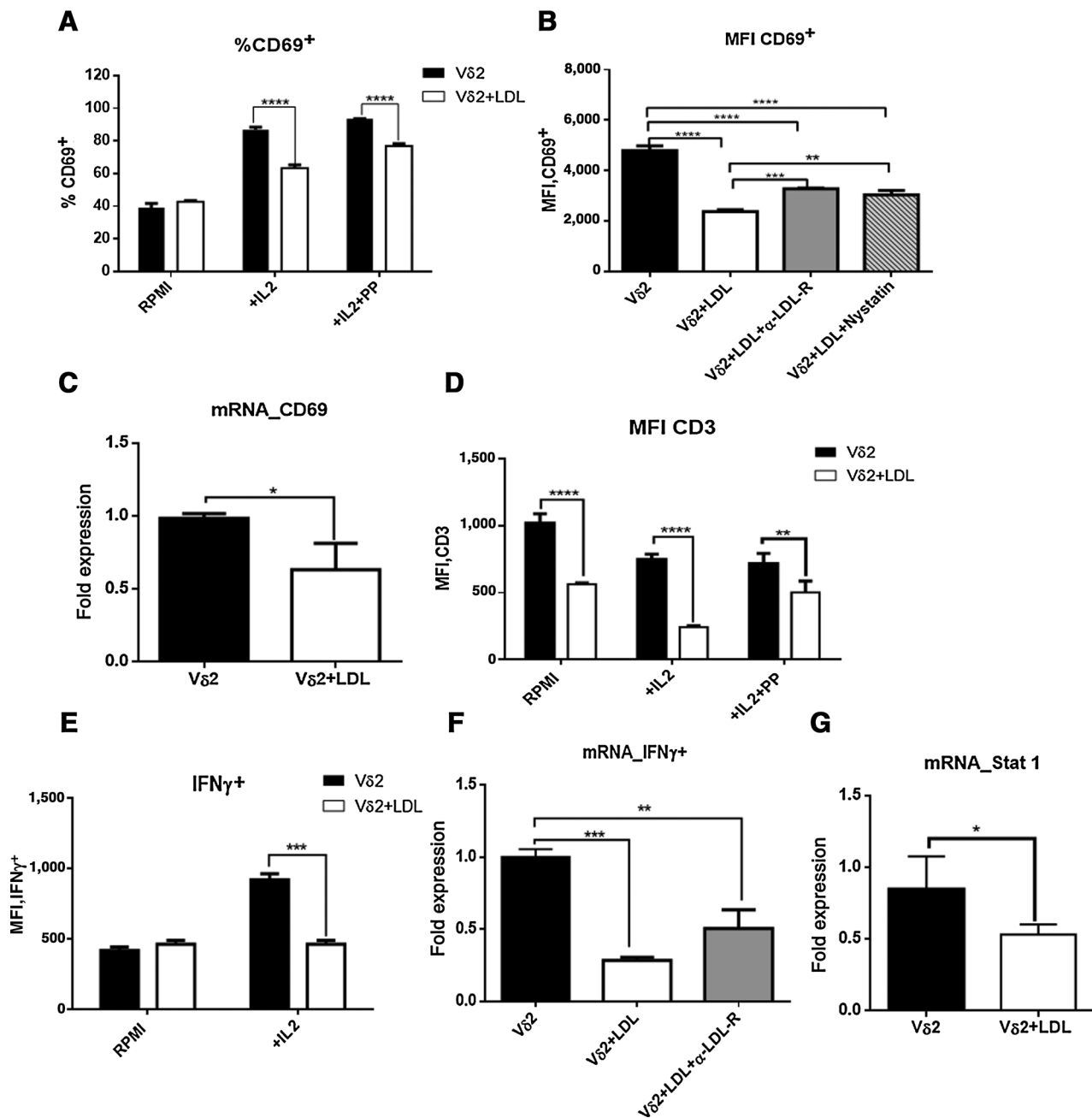


**Figure 2.**

LDL cholesterol inhibits V $\gamma$ 9V $\delta$ 2 T-cell activation and cytokine production. Preexpanded  $\gamma\delta$  (~80% V $\delta$ 2<sup>+</sup>) T cells were cultured in the absence (V $\delta$ 2) or presence of LDL cholesterol (V $\delta$ 2 + LDL) for 72 hours. **A–B**, Percentage of CD69<sup>+</sup> V $\gamma$ 9V $\delta$ 2 T cells (**A**) and MFI for CD69 expression (**B**), in the absence or presence of LDL and, when indicated, anti-LDL-R or Nystatin. **C**, RT-qPCR analysis of the mRNA expression of *CD69*, normalized to the housekeeping gene  *$\beta$ 2-microglobulin*. **D**, MFI for CD3 surface expression. **E**, MFI for intracellular IFN $\gamma$  expression. **F–G**, RT-qPCR analysis of the mRNA expression of *IFN $\gamma$*  (**F**) and *STAT-1* (**G**) normalized to the housekeeping gene  *$\beta$ 2-microglobulin*. Data are from 3 independent experiments and are presented as mean  $\pm$  SD. \*,  $P < 0.05$ ; \*\*,  $P < 0.01$ ; \*\*\*,  $P < 0.001$ , 2-tailed Student *t* test.

upon exposure to LDL may enable V $\gamma$ 9V $\delta$ 2 T cells to limit toxic intracellular accumulation of cholesterol (42). Thus, when V $\gamma$ 9V $\delta$ 2 T cells exposed to LDL were treated with an LDL-R neutralizing antibody, or with Nystatin (a cholesterol-sequestering agent), their activation status was rescued. In contrast, in a mouse model of melanoma, inhibition of cholesterol esterification on

CD8<sup>+</sup> tumor infiltrating T lymphocytes by genetic ablation or pharmacologic inhibition of ACAT1 (a cholesterol esterification enzyme) led to more cholesterol in the plasma membrane, potentiated the antitumor effector function, and enhanced proliferation of CD8<sup>+</sup> T cells (28). That both too little and too much cholesterol causes problems suggests that an optimal

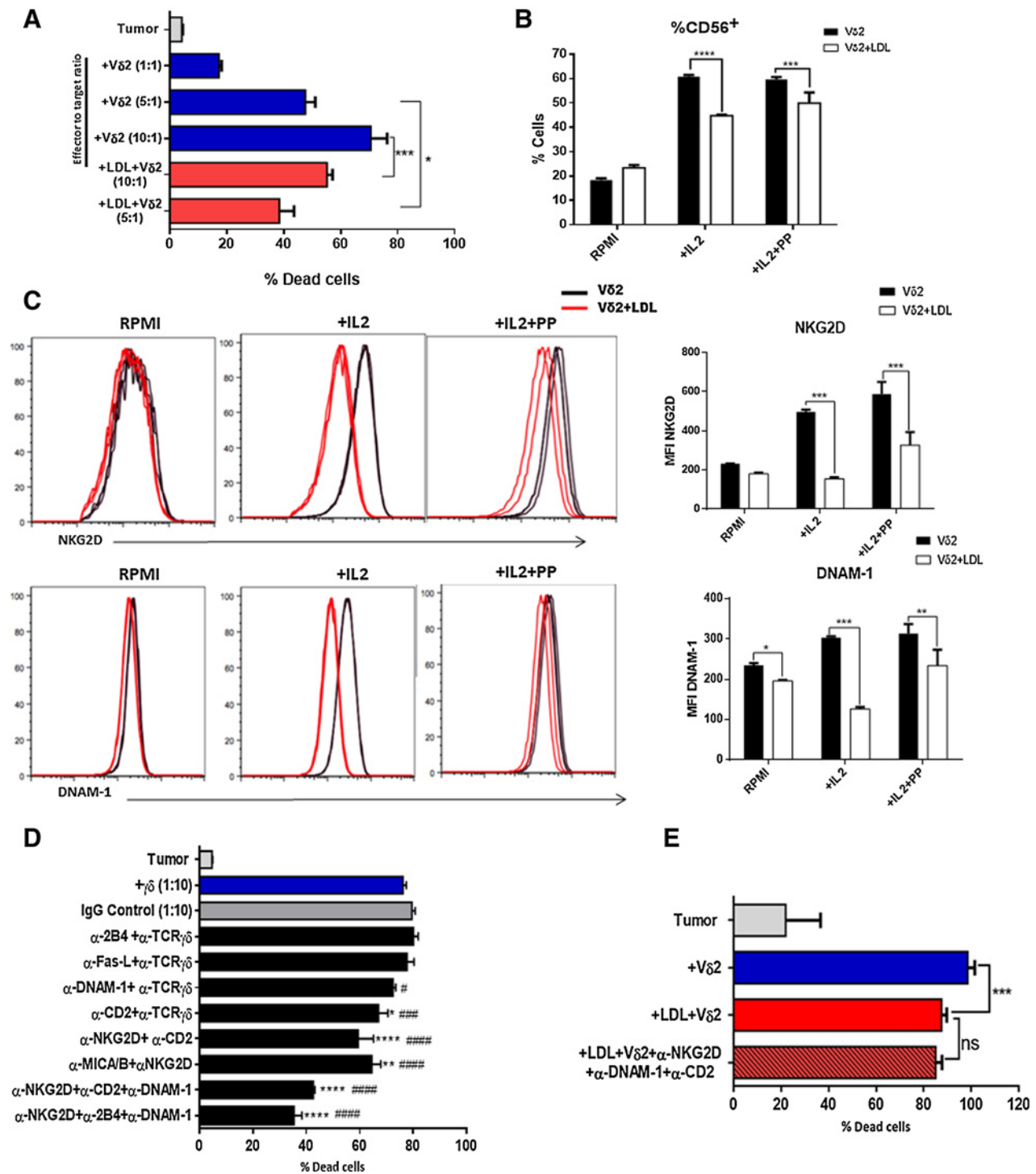


**Figure 3.** LDL cholesterol downregulates NKG2D and DNAM-1 and reduces  $\gamma\delta$  T-cell cytotoxicity *in vitro*. Preexpanded  $\gamma\delta$  (~80% Vδ2<sup>+</sup>) T cells were cultured in the absence (Vδ2) or presence of LDL cholesterol (Vδ2 + LDL) for 72 hours. **A**, *In vitro* killing assays upon coculture for 3 hours with the human breast cancer cell line MDA-MB-231 (at 1:1, 5:1, 10:1 effector:target ratios). The death of target cells (prelabeled with DDAO-SE dye) was assessed by Annexin V staining and flow cytometry. **B**, Percentage of CD56 surface expression. **C**, Expression of the cytotoxicity receptors, NKG2D (top) and DNAM-1 (bottom) determined by flow cytometry, depicted as representative histograms (left) and quantification (MFI, right). **D**, Effect of combinations of blocking antibodies against surface receptors in *in vitro* killing assays with Vγ9Vδ2 T cells cocultured for 3 hours with MDA-MB-231 breast cancer cells at 10:1 effector:target. **E**, Effect of the combination of blocking antibodies against NKG2D, DNAM-1, and CD2 ion LDL exposed Vγ9Vδ2 T cells cocultured with MDA-MB-231 at 10:1 effector:target ratio. The death of target cells (prelabeled with DDAO-SE dye) was assessed by Annexin V staining and flow cytometry. Data are representative of 3 independent experiments and are presented as mean ± SD. \* and # indicate significant differences relative to IgG isotype control or  $\gamma\delta$ , respectively. \*, #, *P* < 0.05; \*\*, ##, *P* < 0.01; \*\*\*, ###, *P* < 0.001.

Downloaded from http://aacrjournals.org/cancerimmunolres/article-pdf/6/4/448/2352673/448.pdf by Institute of Cancer Research user on 14 January 2026

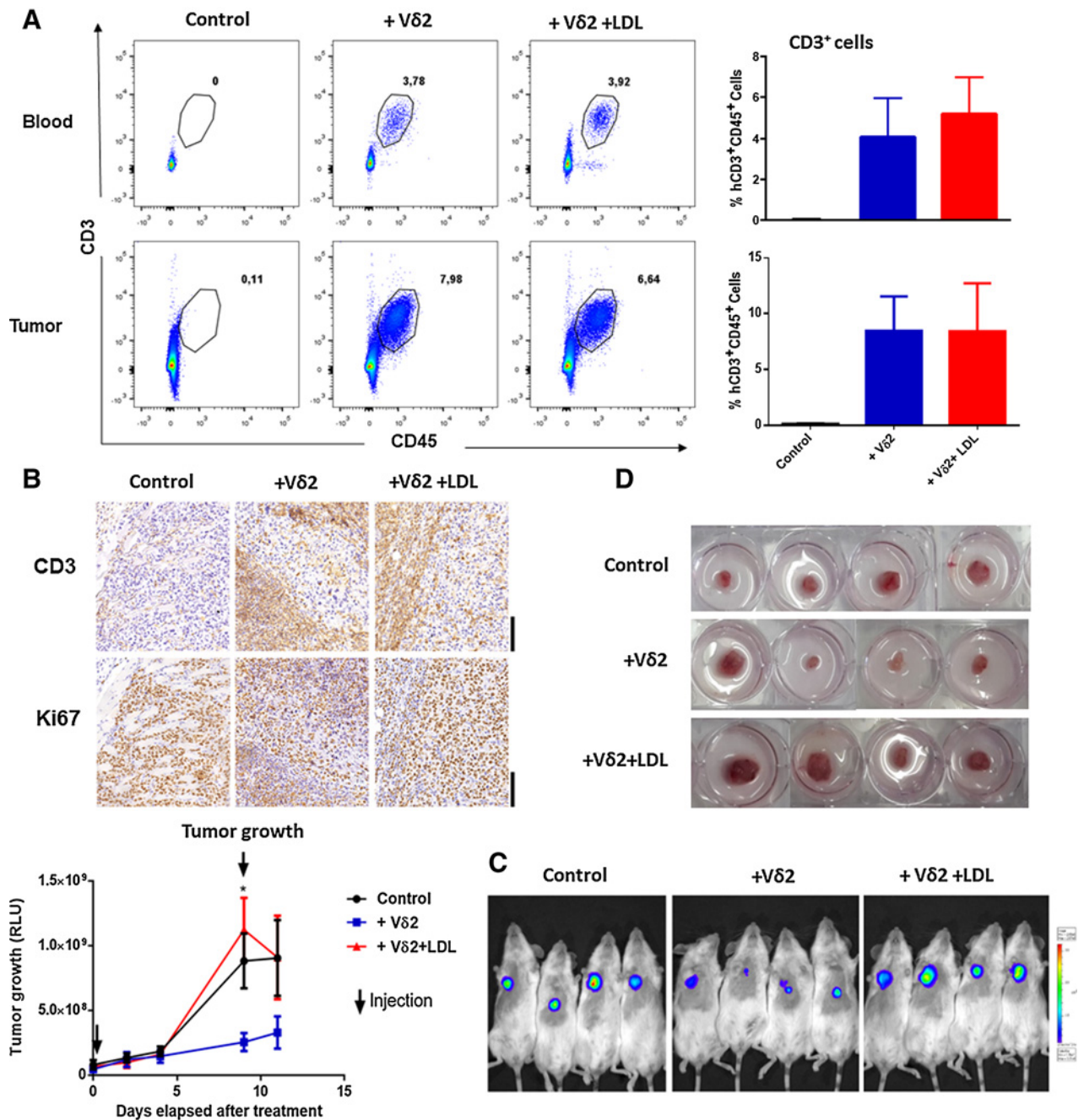


**Figure 4.** LDL cholesterol limits the antitumor therapeutic effect of human  $\gamma\delta$  T cells *in vivo*. NSG mice were injected with  $10^6$  human breast cancer MDA-MB-231 luciferase<sup>+</sup> cells and, after tumor was fully established (day 17), preexpanded V $\delta$ 2 T cells untreated (V $\delta$ 2) or treated with LDL cholesterol (V $\delta$ 2 + LDL), or PBS (as control), were injected twice. At the end of the experiment, animals were sacrificed and organ, tumor and blood were collected for analysis. **A**, Flow cytometry analysis of T cells (CD45<sup>+</sup> CD3<sup>+</sup>) in blood and tumor mass in mice from the different experimental groups. **B**, Immunohistochemistry microphotographs for CD3 and Ki67 in subcutaneous tumors; DAB counterstained with Harris hematoxylin. Original magnification, 20 $\times$  (bar, 100  $\mu$ m). **C**, MDA-MB-231 tumor-bearing NSG mice ( $n = 4$  per group) were analyzed by IVIS Lumina imager. Representative pictures of bioluminescence imaging at terminus and temporal evaluation/quantification along the experiment. **D**, Representative images of the tumors dissected at the end of the experiment. Data are presented as mean  $\pm$  SD. \*,  $P < 0.05$ ; \*\*,  $P < 0.01$ ; \*\*\*,  $P < 0.001$ .

content of intracellular cholesterol is necessary to support T-cell functions. Indeed, free fatty acid uptake and usage by mitochondrial oxidative metabolism supports long-term persistence

of tissue-resident memory CD8<sup>+</sup> T cells (which are generated in response to viral infection) in the skin (43). The inhibitory effects of LDL cholesterol on V $\gamma$ 9V $\delta$ 2 T cells that we study here suggest a

threshold for intracellular lipid accumulation in T cells, beyond which cellular physiology changes. Distinct T-cell subsets may have different sensitivities to cholesterol and different mechanisms to adjust their physiology.

The link between cellular metabolism and regulation of immune cell function has been under study. If TILs cannot sustain mitochondrial function, their effector function is compromised. Studies have suggested that rescuing mitochondrial biogenesis in effector T cells could augment their antitumor immunity (44, 45). We showed here that V $\gamma$ 9V $\delta$ 2 T cells exposed to LDL cholesterol have less mitochondrial DNA and reduced mitochondrial content, changes accompanied by a decrease in ATP production. How a decrease in mitochondrial content and function affects the activation of effector T cells, including V $\gamma$ 9V $\delta$ 2 T cells, remains to be understood. The linkage between cholesterol and cellular metabolism does not hold for all cell types: metabolism of CD8<sup>+</sup> T cells remained unchanged upon inhibition of ACAT1, even after an increase in intracellular cholesterol levels (28).

V $\gamma$ 9V $\delta$ 2 T cells exposed to LDL cholesterol showed impaired production of IFN $\gamma$ , a determinant of V $\gamma$ 9V $\delta$ 2 T-cell antitumor responses (1, 46). We showed that LDL cholesterol reduces the expression of Stat-1, which regulates production of IFN $\gamma$  expression by  $\gamma\delta$  T cells (47). Cholesterol depletion increases V $\gamma$ 9V $\delta$ 2 T-cell cytotoxicity against PC-3 prostate cancer cells by a different mechanism, the upregulation of the mevalonate pathway on target cells (48). Elevated cholesterol levels (hypercholesterolemia) downregulate Tet1 in hematopoietic stem cells, leading to the inhibition of NKT and  $\gamma\delta$  T-cell differentiation and increased colorectal cancer incidence (49). Here, we found a reduction in multifunctional IFN $\gamma$ <sup>+</sup> TNF $\alpha$ <sup>+</sup>  $\gamma\delta$  T cells infiltrating tumor lesions in the syngeneic E0771 model of breast cancer (Supplementary Fig. S6).

Our work showed that expression of the cytotoxicity-associated receptors NKG2D and DNAM-1, which determine tumor susceptibility to  $\gamma\delta$  T cell-mediated cytotoxicity, was downregulated upon exposure of V $\gamma$ 9V $\delta$ 2 T cells to LDL. This occurred in preexpanded/activated V $\gamma$ 9V $\delta$ 2 T cells kept on either IL2 alone or IL2 combined with HMB-PP, thus showing that phosphoantigen stimulation was not able to compensate for the inhibitory effect of LDL on V $\gamma$ 9V $\delta$ 2 T-cell activation. Thus, LDL interferes with the two stages of V $\gamma$ 9V $\delta$ 2 T-cell functionality (18): (i) TCR-mediated activation (as indicated by impaired CD69 and IFN $\gamma$  production), and (ii) NK receptor-mediated tumor targeting (via downregulation of NKG2D and DNAM-1). We showed that the *in vitro* effects of LDL cholesterol on V $\gamma$ 9V $\delta$ 2 T-cell functions were reflected as a loss of their therapeutic effects *in situ* in the xenograft model of human breast cancer.

Taken together, our findings show how tumors may evade immune surveillance in the context of hypercholesterolemia. Chronic lymphocytic leukemia (CLL) patients, who show a high incidence of elevated LDL cholesterol, also show improved survival statistics in response to treatment with cholesterol-lowering

statin drugs (50). Prospective clinical trials are needed to confirm the therapeutic potential of lowering LDL concentrations in CLL and other cancer types. We propose that upcoming research should investigate the linkage between LDL cholesterol levels and survival in the context of the various cancer immunotherapy strategies being evaluated in the clinic.

### Disclosure of Potential Conflicts of Interest

A.C. Hayday is a board member for, reports receiving a commercial research grant from, and has ownership interest in Gamma Delta Therapeutics, and is a consultant/advisory board member for Lycera. No potential conflicts of interest were disclosed by the other authors.

### Authors' Contributions

**Conception and design:** N.V. Rodrigues, A. deBarros, A.C. Hayday, H. Norell, B. Silva-Santos, S. Dias

**Development of methodology:** N.V. Rodrigues, S. Mensurado, S. Nóbrega-Pereira, A. deBarros, H. Norell

**Acquisition of data (provided animals, acquired and managed patients, provided facilities, etc.):** N.V. Rodrigues, D.V. Correia, S. Mensurado, A. deBarros, F. Kyle-Cezar, A. Tutt, A.C. Hayday

**Analysis and interpretation of data (e.g., statistical analysis, biostatistics, computational analysis):** N.V. Rodrigues, D.V. Correia, S. Mensurado, A. deBarros, F. Kyle-Cezar, A.C. Hayday, S. Dias

**Writing, review, and/or revision of the manuscript:** N.V. Rodrigues, S. Nóbrega-Pereira, F. Kyle-Cezar, H. Norell, B. Silva-Santos, S. Dias

**Administrative, technical, or material support (i.e., reporting or organizing data, constructing databases):** N.V. Rodrigues, A.C. Hayday

**Study supervision:** B. Silva-Santos, S. Dias

### Acknowledgments

The study was supported by Fundação para a Ciência e Tecnologia grants: PTDC/DTP-PIC/4931/2014 to B. Silva-Santos; SFRH/BD/113756/2015 to N.V. Rodrigues; SFRH/BPD/85947/2012 to D.V. Correia; SFRH/BPD/91159/2012 to S. Nóbrega-Pereira; Horizon 2020 (TwinnToInfect; grant agreement no. 692022); and LISBOA-01-0145-FEDER-007391, project cofunded by FEDER, through POR Lisboa 2020 - Programa Operacional Regional de Lisboa, PORTUGAL 2020, and Fundação para a Ciência e a Tecnologia. We acknowledge funding from the NIHR to the Biomedical Research Centre at Guys and St. Thomas's NHS Foundation Trust and King's College London.

We thank, for provision and processing of clinical samples, Sheba Irshad, Angela Clifford, and the staff of the Breast Cancer Now Research Unit, Department of Research Oncology, Guy's Hospital, King's College London; and the staff of the Guy's and St. Thomas's Cancer Biobank. We also thank Tânia Carvalho (Histology and Comparative Pathology Laboratory, IMM Lisboa) for histological analyses; Viriato M'Bana (iMM Lisboa) for help with immunofluorescence analysis; Francisco Caiado, Ana Magalhães, and Karine Serre (iMM Lisboa) for technical input; Natacha Gonçalves-Sousa for administrative assistance; and the staff of the Flow Cytometry and Rodent facilities of IMM Lisboa for valuable technical assistance.

The costs of publication of this article were defrayed in part by the payment of page charges. This article must therefore be hereby marked *advertisement* in accordance with 18 U.S.C. Section 1734 solely to indicate this fact.

Received June 23, 2017; revised November 14, 2017; accepted January 8, 2018; published OnlineFirst January 22, 2018.

### References

- Silva-Santos B, Serre K, Norell H. [gamma][delta] T cells in cancer. *Nat Rev Immunol* 2015;15:683–91.
- Bonneville M, O'Brien RL, Born WK. Gammadelta T cell effector functions: a blend of innate programming and acquired plasticity. *Nat Rev Immunol* 2010;10:467–78.
- Lafont V, Sanchez F, Laprevotte E, Michaud HA, Gros L, Eliaou JF, et al. Plasticity of gammadelta T cells: Impact on the anti-tumor response. *Front Immunol* 2014;5:622.
- Casetti R, Martino A. The plasticity of gamma delta T cells: innate immunity, antigen presentation and new immunotherapy. *Cell Mol Immunol* 2008;5:161–70.
- Tanaka Y, Morita CT, Tanaka Y, Nieves E, Brenner MB, Bloom BR. Natural and synthetic non-peptide antigens recognized by human [gamma][delta] T cells. *Nature* 1995;375:155–8.
- Morita CT, Beckman EM, Bukowski JF, Tanaka Y, Band H, Bloom BR, et al. Direct presentation of nonpeptide prenyl pyrophosphate

- antigens to human gamma delta T cells. *Immunity* 1995;3:495–507.
7. Harly C, Guillaume Y, Nedellec S, Peigne CM, Monkkonen H, Monkkonen J, et al. Key implication of CD277/butyrophilin-3 (BTN3A) in cellular stress sensing by a major human gammadelta T-cell subset. *Blood* 2012;120:2269–79.
  8. Sandstrom A, Peigne CM, Leger A, Crooks JE, Konczak F, Gesnel MC, et al. The intracellular B30.2 domain of butyrophilin 3A1 binds phosphoantigens to mediate activation of human Vgamma9Vdelta2 T cells. *Immunity* 2014;40:490–500.
  9. Vavassori S, Kumar A, Wan GS, Ramanjaneyulu GS, Cavallari M, El Daker S, et al. Butyrophilin 3A1 binds phosphorylated antigens and stimulates human gammadelta T cells. *Nat Immunol* 2013;14:908–16.
  10. Ravens S, Schultze-Florey C, Raha S, Sandrock I, Drenker M, Oberdorfer L, et al. Human [gamma][delta] T cells are quickly reconstituted after stem-cell transplantation and show adaptive clonal expansion in response to viral infection. *Nat Immunol* 2017;18:393–401.
  11. Gober HJ, Kistowska M, Angman L, Jenö P, Mori L, De Libero G. Human T cell receptor gammadelta cells recognize endogenous mevalonate metabolites in tumor cells. *J Exp Med* 2003;197:163–8.
  12. Pauza CD, Cairo C. Evolution and function of the TCR Vgamma9 chain repertoire: it's good to be public. *Cell Immunol* 2015;296:22–30.
  13. Gomes AQ, Correia DV, Grosso AR, Lanca T, Ferreira C, Lacerda JF, et al. Identification of a panel of ten cell surface protein antigens associated with immunotargeting of leukemias and lymphomas by peripheral blood gammadelta T cells. *Haematologica* 2010;95:1397–404.
  14. Giralda S, Fortis C, Belloni D, Ferrero E, Ticozzi P, Sciorati C, et al. MICA expressed by multiple myeloma and monoclonal gammopathy of undetermined significance plasma cells Costimulates pamidronate-activated gammadelta lymphocytes. *Cancer Res* 2005;65:7502–8.
  15. Kong Y, Cao W, Xi X, Ma C, Cui L, He W. The NKG2D ligand ULBP4 binds to TCRgamma9/delta2 and induces cytotoxicity to tumor cells through both TCRgammadelta and NKG2D. *Blood* 2009;114:310–7.
  16. Corvaisier M, Moreau-Aubry A, Diez E, Bennouna J, Mosnier JF, Scotet E, et al. V gamma 9V delta 2 T cell response to colon carcinoma cells. *J Immunol* 2005;175:5481–8.
  17. Toutirais O, Cabillic F, Le Fric G, Salot S, Loyer P, Le Gallo M, et al. DNAX accessory molecule-1 (CD226) promotes human hepatocellular carcinoma cell lysis by Vgamma9Vdelta2 T cells. *Eur J Immunol* 2009;39:1361–8.
  18. Correia DV, Lopes A, Silva-Santos B. Tumor cell recognition by gammadelta T lymphocytes: T-cell receptor vs. NK-cell receptors. *Oncoimmunology* 2013;2:e22892.
  19. Hannani D, Ma Y, Yamazaki T, Dechanet-Merville J, Kroemer G, Zitvogel L. Harnessing gammadelta T cells in anticancer immunotherapy. *Trends Immunol* 2012;33:199–206.
  20. Kunzmann V, Bauer E, Wilhelm M. Gamma/delta T-cell stimulation by pamidronate. *N Engl J Med* 1999;340:737–8.
  21. Lo Presti E, Dieli F, Meraviglia S. Tumor-Infiltrating gammadelta T lymphocytes: pathogenic role, clinical significance, and differential programming in the tumor microenvironment. *Front Immunol* 2014;5:607.
  22. Tosolini M, Pont F, Poupot M, Vergez F, Nicolau-Travers ML, Vermijlen D, et al. Assessment of tumor-infiltrating TCRVgamma9Vdelta2 gammadelta lymphocyte abundance by deconvolution of human cancers microarrays. *Oncoimmunology* 2017;6:e1284723.
  23. Rodrigues dos Santos C, Fonseca I, Dias S, Mendes de Almeida JC. Plasma level of LDL-cholesterol at diagnosis is a predictor factor of breast tumor progression. *BMC Cancer* 2014;14:132.
  24. Hansson GK, Hermansson A. The immune system in atherosclerosis. *Nat Immunol* 2011;12:204–12.
  25. Kidani Y, Bensinger SJ. Modulating cholesterol homeostasis to build a better T cell. *Cell Metab* 2017;23:963–4.
  26. Peng G, Wang HY, Peng W, Kiniwa Y, Seo KH, Wang RF. Tumor-infiltrating gammadelta T cells suppress T and dendritic cell function via mechanisms controlled by a unique toll-like receptor signaling pathway. *Immunity* 2007;27:334–48.
  27. Molnar E, Swamy M, Holzer M, Beck-Garcia K, Worch R, Thiele C, et al. Cholesterol and sphingomyelin drive ligand-independent T-cell antigen receptor nanoclustering. *J Biol Chem* 2012;287:42664–74.
  28. Yang W, Bai Y, Xiong Y, Zhang J, Chen S, Zheng X, et al. Potentiating the antitumor response of CD8+ T cells by modulating cholesterol metabolism. *Nature* 2016;531:651–5.
  29. Sag D, Cekic C, Wu R, Linden J, Hedrick CC. The cholesterol transporter ABCG1 links cholesterol homeostasis and tumour immunity. *Nat Commun* 2015;6:6354.
  30. Rodrigues dos Santos C, Domingues G, Matias Is, Matos Jo, Fonseca I, de Almeida JM, et al. LDL-cholesterol signaling induces breast cancer proliferation and invasion. *Lipids Health Dis* 2014;13:16.
  31. Rooney JP, Ryde IT, Sanders LH, Howlett EH, Colton MD, Germ KE, et al. PCR based determination of mitochondrial DNA copy number in multiple species. *Methods Mol Biol* 2015;1241:23–38.
  32. Pavlova NN, Thompson CB. The emerging hallmarks of cancer metabolism. *Cell Metab* 2016;23:27–47.
  33. Beloribi-Djefailia S, Vasseur S, Guillaumond F. Lipid metabolic reprogramming in cancer cells. *Oncogenesis* 2016;5:e189.
  34. Havas KM, Milchevskaia V, Radic K, Alladin A, Kafkia E, Garcia M, et al. Metabolic shifts in residual breast cancer drive tumor recurrence. *J Clin Invest* 2017;127:2091–105.
  35. Menendez JA, Lupu R. Fatty acid synthase and the lipogenic phenotype in cancer pathogenesis. *Nat Rev Cancer* 2007;7:763–77.
  36. Nieman KM, Kenny HA, Penicka CV, Ladanyi A, Buell-Gutbrod R, Zillhardt MR, et al. Adipocytes promote ovarian cancer metastasis and provide energy for rapid tumor growth. *Nat Med* 2011;17:1498–503.
  37. Uehara H, Takahashi T, Oha M, Ogawa H, Izumi K. Exogenous fatty acid binding protein 4 promotes human prostate cancer cell progression. *Int J Cancer* 2014;135:2558–68.
  38. Condamine T, Dominguez GA, Youn J-I, Kossenkov AV, Mony S, Alicea-Torres K, et al. Lectin-type oxidized LDL receptor-1 distinguishes population of human polymorphonuclear myeloid-derived suppressor cells in cancer patients. *Science Immunol* 2016;1:aaf8943–aaf.
  39. Nelson ER, Wardell SE, Jasper JS, Park S, Suchindran S, Howe MK, et al. 27-Hydroxycholesterol links hypercholesterolemia and breast cancer pathophysiology. *Science* 2013;342:1094–8.
  40. Lingwood D, Simons K. Lipid rafts as a membrane-organizing principle. *Science* 2010;327:46–50.
  41. Sag D, Cekic C, Wu R, Linden J, Hedrick CC. The cholesterol transporter ABCG1 links cholesterol homeostasis and tumour immunity. *Nat Commun* 2015;6:6354.
  42. Zhang K, Kaufman RJ. Unfolding the toxicity of cholesterol. *Nat Cell Biol* 2003;5:769–70.
  43. Pan Y, Tian T, Park CO, Lofftus SY, Mei S, Liu X, et al. Survival of tissue-resident memory T cells requires exogenous lipid uptake and metabolism. *Nature* 2017;543:252–6.
  44. Bengsch B, Johnson AL, Kurachi M, Odorizzi PM, Pauken KE, Attanasio J, et al. Bioenergetic insufficiencies due to metabolic alterations regulated by the inhibitory receptor PD-1 are an early driver of CD8+ T cell exhaustion. *Immunity* 2016;45:358–73.
  45. Scharping NE, Menk AV, Moreci RS, Whetstone RD, Dadey RE, Watkins SC, et al. The tumor microenvironment represses T cell mitochondrial biogenesis to drive intratumoral T cell metabolic insufficiency and dysfunction. *Immunity* 2016;45:701–3.
  46. Hayday AC. Gammadelta T cells and the lymphoid stress-surveillance response. *Immunity* 2009;31:184–96.
  47. Ramana CV, Gil MP, Schreiber RD, Stark GR. Stat1-dependent and -independent pathways in IFN-gamma-dependent signaling. *Trends Immunol* 2002;23:96–101.
  48. Arkko S, Zlatev HP, Monkkonen H, Raikkonen J, Benzaid I, Clezardin P, et al. Upregulation of the mevalonate pathway by cholesterol depletion abolishes tolerance to N-bisphosphonate induced Vgamma9Vdelta2 T cell cytotoxicity in PC-3 prostate cancer cells. *Cancer Lett* 2015;357:279–85.
  49. Tie G, Yan J, Khair L, Messina JA, Deng A, Kang J, et al. Hypercholesterolemia increases colorectal cancer incidence by reducing production of NKT and gammadelta T cells from hematopoietic stem cells. *Cancer Res* 2017;77:2351–62.
  50. McCaw L, Shi Y, Wang G, Li Y-J, Spaner DE. Low density lipoproteins amplify cytokine-signaling in chronic lymphocytic leukemia cells. *EBioMedicine* 2017;15:24–35.